



X-ray spectroscopy of few-electron uranium ions for tests of QED

Louis Duval, Robert Loetzsch, Heinrich F. Beyer, Dariusz Banaś, Perla Dergham, Jan Glorius, Robert Evaristo Grisenti, Mauro Guerra, Alexandre Gumberidze, Pierre-Michel Hillenbrand, et al.

► To cite this version:

Louis Duval, Robert Loetzsch, Heinrich F. Beyer, Dariusz Banaś, Perla Dergham, et al.. X-ray spectroscopy of few-electron uranium ions for tests of QED. 2023. hal-04007983

HAL Id: hal-04007983














<https://hal.science/hal-04007983>

Preprint submitted on 6 Mar 2023

HAL is a multi-disciplinary open access archive for the deposit and dissemination of scientific research documents, whether they are published or not. The documents may come from teaching and research institutions in France or abroad, or from public or private research centers.

L'archive ouverte pluridisciplinaire **HAL**, est destinée au dépôt et à la diffusion de documents scientifiques de niveau recherche, publiés ou non, émanant des établissements d'enseignement et de recherche français ou étrangers, des laboratoires publics ou privés.

X-ray spectroscopy of few-electron uranium ions for tests of QED

 L. Duval,^{a,b,*} R. Loetzsch,^c H. Beyer,^d D. Banaś,^f P. Dergham,^b J. Glorius,^d
R.E. Grisenti,^{d,e}  M. Guerra,^g  A. Gumberidze,^d  P-M. Hillenbrand,^e
P. Jagodziński,^f E. Lamour,^b Y. Litvinov,^d  J. Machado,^g G. Paulus,^c  N. Paul,^a
N. Petridis,^d  J-P. Santos,^f M. Scheidel,^d  R.S. Sidhu,^{d,h,i}  U. Spillmann,^d
S. Steydli,^b K. Szary,^f S. Trotsenko,^d I. Uschmann,^c  G. Weber,^j  T. Stöhlker,^{c,d,j}
 P. Indelicato^a and  M. Trassinelli^b

^aLaboratoire Kastler Brossel, Sorbonne Université, CNRS, ENS-PSL Research University, Collège de France, Case 74; 4, place Jussieu, F-75005 Paris, France

^bInstitut des NanoSciences de Paris, CNRS, Sorbonne Université
4 Place Jussieu, 75005 Paris, France

^cInstitut für Optik und Quantenelektronik, Friedrich-Schiller-Universität, 07737 Jena, Germany

^dGSI Helmholtzzentrum für Schwerionenforschung GmbH, 64291 Darmstadt, Germany

^eInstitut für Kernphysik, Goethe-Universität, 60438 Frankfurt, Germany

^fInstitute of Physics, Jan Kochanowski University, 25-406 Kielce, Poland

^gLaboratório de Instrumentação, Engenharia Biomédica e Física das Radiações, Departamento de Física, Faculdade Ciências e Tecnologia, Universidade Nova de Lisboa, 2829-516 Caparica, Portugal

^hMax-Planck-Institut für Kernphysik, Saupfercheckweg 1, 69117 Heidelberg, Germany

ⁱSUPA, School of Physics and Astronomy, University of Edinburgh, Edinburgh, United Kingdom

^jHelmholtz-Institut Jena, 07743 Jena, Germany

E-mail: louis.duval@lkb.upmc.fr

We present a here a non-parametric analysis of x-ray spectra for experiment E125 performed at GSI-FAIR in Darmstadt. This experiment measured intra-shell transitions of highly charged uranium with a twin-arm Bragg spectrometer equipped with x-rays CCDs. The method consists in slicing the CCD image and calculating the centroids of the lines, then adjusting the slice size in order to remove background. Due to the low count rate, we reveal the limitations of this method which provides an accuracy of only a few pixels, far from the sub-pixel requirement.

FAIR next generation scientists - 7th Edition Workshop (FAIRness2022)
23-27 May 2022
Paralia (Pieria, Greece)

*Speaker

1. Bound-State Quantum Electro-Dynamics (BSQED)

Bound-state quantum electrodynamics (BSQED) describes three fundamental processes in the Coulomb field of the nucleus: the electron-electron interaction, self-energy and vacuum polarization. The electron-electron interaction takes into account the exchange of virtual photons between the electrons, the self energy is the emission and absorption of a virtual photon by the electron, and the vacuum polarization is the creation of a particle-antiparticle pair in the electric field of the nucleus [1] (see Fig.1).

In highly-charged uranium, the second order QED corrections reach ppm contributions and can be tested with available experimental methods. This is goal of the experiment described in the next section.

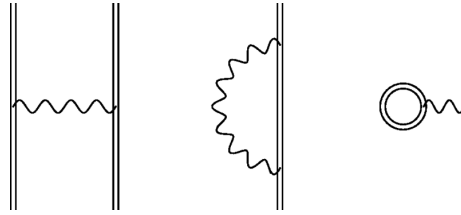


Figure 1: Feynman Diagrams of the 1st order in α . These diagrams allow to calculate corrections from quantum electrodynamics. From left to right: electron-electron interaction, self energy and vacuum polarization. The double line represents an electron in a bound state.

2. Experiment E125

The main goal of the E125 experiment is to measure the difference in energy between the $1s^1 2p^2 P_{3/2} \rightarrow 1s^1 2s^2 S_{1/2}$ transition in Helium-like uranium and the $1s^2 2p^2 P_{1/2} \rightarrow 1s^2 2s^2 S_{1/2}$ transition in Lithium-like uranium, following the same strategy as the past experiment described in Ref. [2]. During this campaign, the transition $1s^2 2p^2 ^1P_1 \rightarrow 1s^2 2s^2 ^1S_0$ of the Be-like uranium has also been studied. These measurements allow to access the $2s - 2p$ Lamb shift [3, 4] for different charge states. Using Be- and Li-like uranium as reference, the intrashell transition in He-like uranium can be measured with high accuracy, sufficient to be sensitive to second-order one-electron QED effects. When the differences in energy of intrashell transitions from different charge states is considered, two-electron QED effects in intense Coulomb field regime can also be tested.

2.1 Experimental Setup and Measurement

In E125, bunches of 10^8 H-like, He-like and Li-like uranium ions were injected into the Experimental Storage Ring of GSI. After the deceleration and the cooling of the bunch [5] of about 4×10^8 ions, a 5 mm wide nitrogen gas jet, with a density of 10^{12} atoms/cm², is turned on [6]. By colliding with the gas jet, the highly charged ions capture one electron in an excited level. The excited states decay and produce photons that are Bragg-deflected thanks to two curved Ge(220) crystals placed at observational angles of $\pm 90^\circ$ with respect to the ion beam direction. The photons are collected with position-sensitive x-ray CCDs. Thus, we obtain raw images such as the one presented in Fig. 2, for the x rays of the $1s^2 2p^3 P_{3/2} \rightarrow 1s^2 2p^3 S_{1/2}$ transition in Li-like uranium with one of the spectrometer x-ray CCDs.

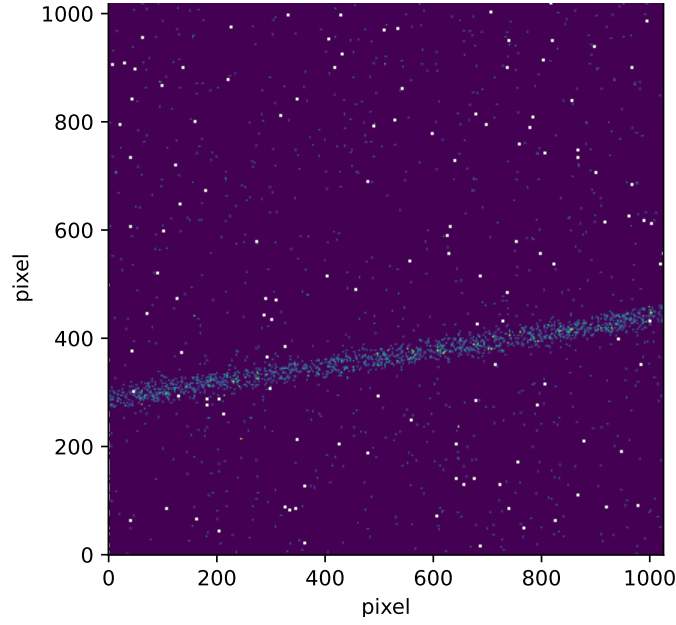


Figure 2: Image from Li-like uranium with *Great Eyes* CCD. The dark background corresponds to pixels with no counts inside. The clear blue points correspond to pixels which have received 1 or 2 counts and the white points are the dead pixels.

2.2 Experimental methodology

Since the energy window of the Bragg spectrometer is too narrow (~ 30 eV) to measure all the transitions at once, the Doppler effect is used to set all the energies in the laboratory frame to be approximately equal.

The observation angle is set to 90° such that $E_{\text{laboratory}} = E_{\text{transition}}/\gamma$. The Bragg angle is chosen to have the reflection of a stationary calibration source almost coinciding with the Doppler shifted ion x-ray reflections. For this purpose, on the one hand the ion transitions were shifted to the energy of 4319 eV and reflected at first-order at the angle of 45.85° . On the other hand, the zinc $K\alpha_1$ fluorescence line, corresponding to 8638 eV photons and reflected at the second-order, was chosen as stationary reference with $\gamma = 2E_{\text{transition}}/E_{\text{calibration}}$. The Lorentz factor γ is experimentally set by the high voltage of the electron cooler that imposes the velocity of the ions.

The Lorentz factor γ , the β factor and the energy of the beam are related to each other through the following relationships

$$\beta = \sqrt{1 - \frac{1}{\gamma^2}}, \quad E_{\text{beam}} = m_{\text{nucleon}}(\gamma - 1), \quad (1)$$

where $m_{\text{nucleon}} = 931.494 \text{ MeV}/c^2$ [7]. The values are given in Table 1.

2.3 Position of the line on the CCD

As the uranium ions are travelling at around 25% of the speed of light (*cf* Table 1), the Doppler effect changes the energy in the laboratory frame, depending on the observation angle α of the photon and the speed of the uranium beam according to:

Charge State	$E_{\text{transition}}$ (eV)	γ	β	Energy per nucleon (MeV)	Angle ($^\circ$)
Be-like [8]	4501.72(21)	1.04220	0.281671	39.29	10.17
Li-like [8]	4459.37(27)	1.03239	0.248533	30.16	8.83
He-like [9]	4509.80(99)	1.04407	0.287462	41.04	10.42
Zinc $K\alpha_1$ [10]	8638.906(73)	1	0	0 (x-ray tube)	0

Table 1: Experimental transition energies, Lorentz factor γ , β (both defined in Eq. (1)) and beam energies needed to observe the transitions in the spectrometer (Bragg angle = 45.85°). The angles of the lines on the CCD are also given.

$$E_{\text{transition}} = \frac{hc}{2d \sin(\theta)} \gamma (1 - \beta \cos(\alpha)) \quad (2)$$

The photon is Bragg deflected by the crystal. Its position on the CCD, taking its middle as the reference frame, with r_{source} the distance between the crystal and the interaction point, r_{CCD} the distance between the crystal and the CCD and $\theta_0 = 90^\circ - \alpha$, is:

$$\begin{pmatrix} \Delta x \\ \Delta z \end{pmatrix} = \begin{pmatrix} r_{\text{CCD}} \tan(\theta_{\text{bragg photon}} - \theta_{\text{bragg ref}}) \\ (r_{\text{source}} + r_{\text{CCD}}) \cot(\theta_0) \end{pmatrix}, \quad (3)$$

We can determine the angle of the line ϕ_{line} on the CCD via

$$\phi_{\text{line}}(\alpha) = \text{arccot}\left(\frac{\Delta x}{\Delta z}\right) \quad (4)$$

With respect to the overall size of the CCD, the angle of the line changes by less than 0.01° , which represents a deviation of the line smaller than 0.01 pixel over the CCD. Thus, the angle of the line is considered as constant over the CCD. The angles calculated are reported in Table 1.

2.4 Analysis of the lines

Due to the presence of noise on the CCD images, a background-rejection method had to be used. Either a non-parametric approach or a parametric model of the line has to be chosen. In this experiment, both approaches have been tested. Here only a non-parametric approach is presented. In order to determine the position of the line and its angle, a centroid approach is used. The centroid of the photon distribution in the X-Y plane of the CCD, produced by the decay is considered as the position of the line. With this position we can obtain the energy of the transition thanks to the Bragg dispersion relation: $2d \sin \theta = n\lambda$.

The algorithm works as follows:

1. Dead pixel weights are set to 0.
2. The image is sliced vertically, with a given number of slices.
3. A centroid (\bar{x}, \bar{y}) and standard deviation calculation (σ_x, σ_y) is performed in each slice.
4. A new vertical window is defined in each slice: $[\bar{y} - \epsilon \times \sigma_y ; \bar{y} + \epsilon \times \sigma_y]$, where ϵ is chosen to optimize both convergence and precision.

5. The centroid and standard deviation calculation is performed in the slice with the new vertical window.
6. The centroid calculation stops when every centroid changes by less than a pixel or the standard deviation is too small.
7. The centroid list is fitted with a χ^2 method, giving the position and the angle of the line.

An example of the algorithm output is shown in Fig. 3.

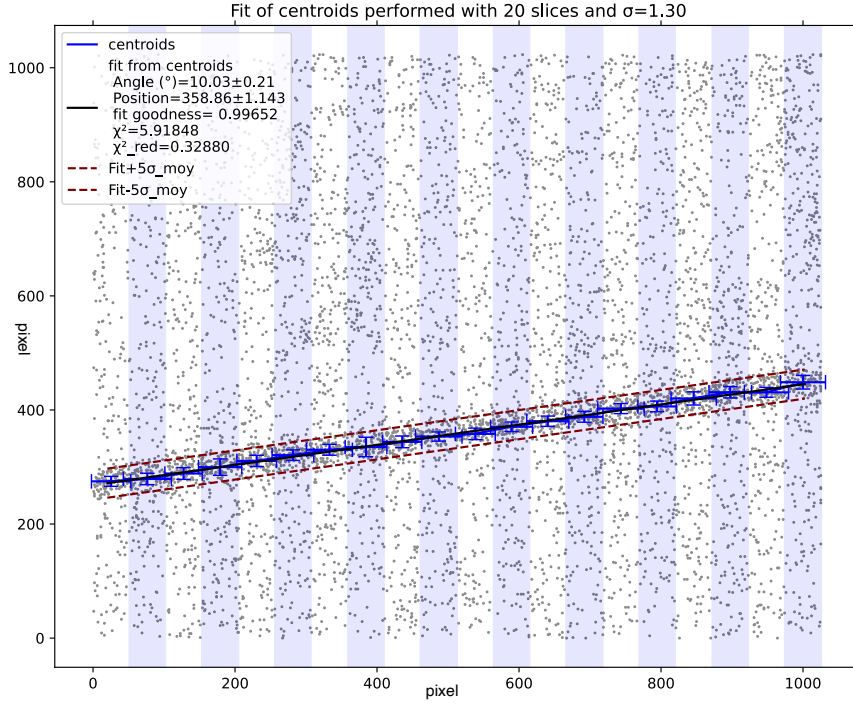


Figure 3: Centroids and fit of centroids obtained with the centroid determination algorithm using as input parameters $\epsilon = 1.3$ and 20 slices for the He-like Uranium run. Uncertainties plotted corresponds to 2σ , slices are shown within the background.

2.5 Fitting results

Once the algorithm is done running, the results are stored and are compared in order to check if all the results are compatible among different input parameters of the algorithm. From there, a weighted average of the line position is calculated. The arithmetical mean of the standard deviations is used as the uncertainty when performing the average. We can see notable systematic effects for the position and the angle of the line like in Fig. 4. Indeed, if ϵ is chosen too small, the algorithm will reduce quickly the window and may converge out of the line; too big would result in a new window larger than the new image. If the number of the slices is too big, the number of counts inside the slice will be not enough to allow a correct centroid calculation. These dependencies can also be understood from the fact that every centroid calculated is affected by noise, which is not cancelled by the fitting method.

This non-parametric approach, with a low signal-to-noise ratio, can only be used to have a first guess of the line position, but getting a sub-pixel uncertainty seems not reachable as referenced in

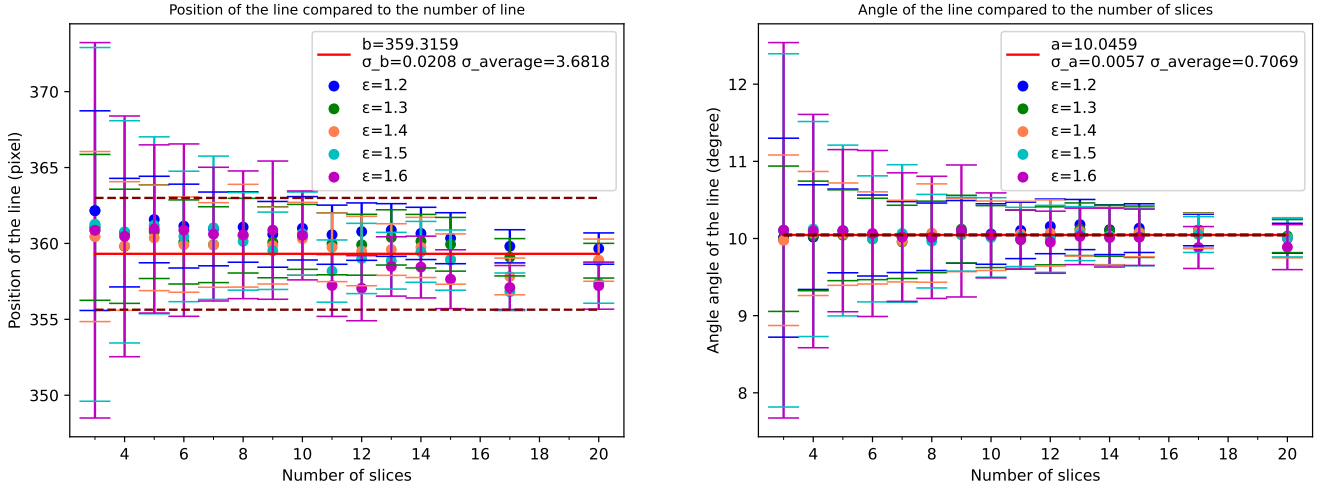


Figure 4: Position of the line (left) and angle of the line (right) for the right arm depending on the input parameters of the algorithm, for the He-like Uranium. The fitting (red) is done with a χ^2 method. The uncertainty of the final value is the mean of all the standard deviations in the plot.

Table 2. Indeed, as the count occupation within the line is 4%, a minimum size of a several pixels has to be defined to get at least 2 counts (minimum necessary to be able to calculate the variance around the centroid), making the dispersion around the centroid wider than a pixel.

With a higher signal-to-noise ratio and a higher count rate, the method is probably more efficient, even if the systematic effects still affect the determination of the parameters, but with a clearly reduced amplitude.

Arm	Line	Position (pixel)	angle (degree)
Left	zinc $K\alpha_1$ calibration for Li-like run	710(1)	-0.7(1)
	Li-like	792(3)	-9.2(3)
	zinc $K\alpha_1$ calibration for He-like	710(1)	-0.7(1)
	He-like	805(3)	-11.0(3)
	zinc $K\alpha_1$ calibration for Be-like run	710(1)	-0.7(1)
	Be-like	806(3)	-10.7(3)
Right	zinc $K\alpha_1$ calibration for Li-like run	388(1)	-0.3(2)
	Li-like	364(3)	8.5(6)
	zinc $K\alpha_1$ calibration for He-like run	389(1)	-0.3(2)
	He-like	359(3)	10.1(6)
	zinc $K\alpha_1$ calibration for Be-like run	389(1)	-0.3(2)
	Be-like	360(3)	9.6(5)

Table 2: Position and angle of the line for all the images taken during E125

3. Conclusion

Experiment E125, performed in May 2021 at GSI-FAIR, measured the $1s^1 2p \ ^2P_{3/2} \rightarrow 1s^1 2s \ ^2S_{1/2}$ transition in He-like uranium, in order to probe 2nd order QED effects. The x-ray

transition energy measurement was based on Bragg spectroscopy using a crystal spectrometer. In this work, we tested a non-parametric approach for the determination of the line position. We showed that this approach determines the line position with a precision of around 3 pixels, which does not meet the requirement of a sub-pixel precision. Such an accuracy is obtained from a parametric analysis that will be presented in a future publication.

Acknowledgments

The results presented here are based on the experiment E125, which was performed at the infrastructure ESR at the GSI Helmholtzzentrum für Schwerionenforschung, Darmstadt (Germany) in the frame of FAIR Phase-0. This work has been supported by the European Union's Horizon 2020 research and innovation programme und grant agreement n° 6544002. M.T. thanks in addition the ExtreMe Matter Institute and Alexander von Humboldt Foundation for their support for the stays at the GSI for the preparation and data acquisition. We acknowledge substantial support by ErUM-FSP APPA (BMBF n° 05P19SJFAA). P. J. acknowledges funding support from National Science Centre, Poland, grant number DEC-2022/06/X/ST2/00453. L. D. acknowledges funding support from the Initiative Physique des Infinis (IPI), a research training program of the Ixex SUPER at Sorbonne Université

References

- [1] H.F. Beyer and V.P. Shevelko, *Introduction to the physics of highly charged ions*, vol. 500, CRC Press (4, 2002), [10.1016/s0168-9002\(03\)00733-2](https://doi.org/10.1016/s0168-9002(03)00733-2).
- [2] M. Trassinelli, *Bayesian Data Analysis Tools for Atomic Physics*, *Nucl. Instr. Methods B* **408** (2017) 301.
- [3] W.E. Lamb and R.C. Retherford, *Fine Structure of the Hydrogen Atom by a Microwave Method*, *Phys. Rev.* **72** (1947) 241.
- [4] P. Indelicato, *Topical Review: QED Tests with Highly-Charged Ions*, *J. Phys. B: At. Mol. Opt. Phys.* **52** (2019) 232001.
- [5] M. Steck and Y.A. Litvinov, *Heavy-Ion Storage Rings and Their Use in Precision Experiments with Highly Charged Ions*, *Prog. Part. Nucl. Phys.* **115** (2020) 103811.
- [6] N. Petridis, R.E. Grisenti, Y.A. Litvinov and T. Stöhlker, *Prototype Internal Target Design for Storage Ring Experiments*, *Phys. Scr.* **T166** (2015) 014051.
- [7] E. Tiesinga, P.J. Mohr, D.B. Newell and B.N. Taylor, *Codata Recommended Values of the Fundamental Physical Constants: 2018*, *Rev. Mod. Phys.* **93** (2021) 025010.
- [8] P. Beiersdorfer, D. Knapp, R. Marrs, S. Elliot and M. Chen, *Structure and Lamb-Shift of $2s_{1/2} - 2p_{3/2}$ Levels in Lithiumlike U^{89+} through Neonlike U^{82+}* , *Phys. Rev. Lett.* **71** (1993) 3939.

- [9] M. Trassinelli, A. Kumar, H. Beyer, P. Indelicato, R. Märtin, R. Reuschl et al., *Observation of the $^2P_{3/2} \rightarrow ^2S_{1/2}$ Intra-Shell Transition in He-Like Uranium*, *Eur. Phys. Lett.* **87** (2009) 63001 (6).
- [10] R. Deslattes, E.K. Jr., P. Indelicato, L. de Billy, E. Lindroth and J. Anton, *X-Ray Transition Energies: New Approach to a Comprehensive Evaluation*, *Rev. Mod. Phys.* **75** (2003) 35.